AENSI Journals

**Advances in Environmental Biology**

ISSN-1995-0756 EISSN-1998-1066

Journal home page: http://www.aensiweb.com/AEB/

# Simulation and Calculation of the Parameters of PCF under Terahertz Wave Band

**[1]A. Afroozeh, [2,3]S.E. Pourmand, [4]A. Zeinalinezhad**

*[1]Young Researchers and Elite Club, Jahrom Branch, Islamic Azad University, Jahrom, Iran.*
*[2]Department of Optics and Lasers Engineering, Estahban Branch, Islamic Azad University, Estahban, Iran.*
*[3]Young Researchers and Elite Club, Estahban Branch, Islamic Azad University, Estahban, Iran.*
*[4]Chemistry Department, Anar Branch, Islamic Azad University, Anar, Iran.*

**ARTICLE INFO**

***Article history:***
*Received 4 September 2014*
*Received in revised form 24 November 2014*
*Accepted 8 December 2014*
*Available online 16 December 2014*

***Keywords:***
*Terahertz wave, photonic crystal fiber, Liquid Crystal*

**ABSTRACT**

**Background:** This manuscript shows a new structure of photonic crystal fiber (PCF). Here, the finite element method has been used to simulated the conditions that the modes of the PCF which have continuously modifiable sensing properties by filling with nematic liquid crystal (LC). In this study, software of COMSOL and MATLAB has been to simulation and calculation of the parameters of PCF under THZ wave band from 0.1 THZ to 10 THZ.



**To Cite This Article:** A. Afroozeh, S. E. Pourmand, A. Zeinalinezhadhors., Simulation and Calculation of the Parameters of PCF under Terahertz Wave Band. ***Adv. Environ. Biol., 8(21),*** *263-268, 2014*

## INTRODUCTION

A PCF is an optical fiber that achieves its waveguide properties not from a spatially variable glass structure but from planning of very small and closely spaced air holes which go through the whole length of fiber [1-3]. Photonic-crystal fiber (PCF) is a novel class of optical fiber based on the properties of photonic crystals. Because of its ability to confine light in hollow cores or with confinement characteristics not possible in conventional optical fiber, PCF is now finding applications in fiber optic communications, fiber lasers, nonlinear devices, high-power transmission, highly sensitive gas sensors and other areas [4, 5]. Additional specific classes of PCF include photonic band gap fiber, holey fiber, hole-assisted fiber and Bragg fiber [6, 7]. PCF fibers may be measured a subcategory of a more general class of micro structured optical fibers, where light is directed by essential adjustments and not only by refractive index differences [8]. The PCF can freely control the motion of photons which give us a lot of room for designing and constructing, making PCF possess many more attractive features than electron crystal material. It gave a technology and has become a big hot spot in photoelectron research in recent years [9, 10]. Terahertz wave frequency range is 0.1THz~10THz, located midway between the microwaves infrared light. This bandwidth is also recognized as the THZ gap because it is noticeably underutilized. Because terahertz waves are electromagnetic waves with frequencies higher than microwaves but lower than. infrared radiation and visible light. PCF applied in THZ bands has the advantage of easy preparation and etc. because its size is in millimeters magnitude [11-17]. The reaction of the refractive index of LC to the change of the external electric field is more sensitive than others, so we can adjust the parameters of the PCF through infiltrating the air holes with the LC selectively and changing the voltage of applied electric field [18, 19].

*Refractive Index of Lc:*

LC is an intermediate state between liquid and crystal, also called the fourth state of substance. A liquid crystal having both the flow ability and orderly crystal-like structure, it like liquid on the mechanical properties and like the crystal on the optical properties, so we also called it liquid crystal [20]. In this paper, heating cyanobiphenyl (CB) nematic liquid crystal (LC) and change the refractive index of LC By changing the external electric field have been used. When there is no applied electric field, the LC molecules are similar to the uniaxial crystal. The direction of Z axis is consistent with the direction of LC molecular alignment as shown in Figure 1. It's equivalent that light spread in the isotropic material, so the transmitted light is ordinary light and

**Corresponding Author:** Abdolkarim Afroozeh, Young Researchers and Elite Club, Jahrom Branch, Islamic Azad University, Jahrom, Iran.
E-mail: afroozeh155@yahoo.com.

the refractive index of LC is no. When the applied voltage is greater than the threshold voltage, the LC molecules will begin to spin. The angle between long axis's direction of LC molecules and PCF axis direction is θ as shown in Figure 2. It's similar as that light spread in the anisotropic medium. In the process of voltage increase, the polarized light in X axis direction will keep unchanged light refractive index. The polarized light in Y axis direction will change with the impressed voltage [21, 22].

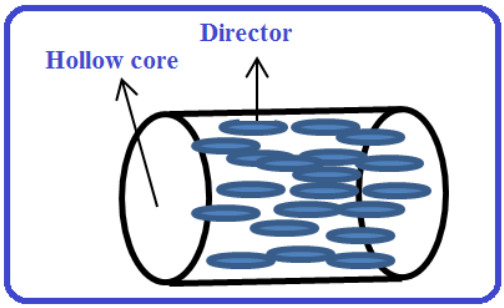


**Fig. 1:** The orientation of the LC molecules, for E=0

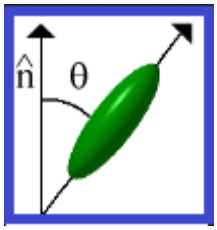


**Fig. 2:** The orientation of the LC molecules for E≠0

The polarized refractive index of LC molecules in the direction along the X-axis and Y-axis can be obtained by the following formula [23, 24]:

$$n_x = n_0 \tag{1}$$

$$n_y = \left(\frac{\sin^2\theta}{{n_e}^2} + \frac{\cos^2\theta}{{n_o}^2}\right)^{-\frac{1}{2}} \tag{2}$$

The refractive index of extraordinary light and ordinary light of LC 5CB at 25 °C are around 1.77 and 1.58 in the frequency range of 0.2 to 1.0 THz, respectively [25, 26] where θ is determined by:

$$\theta = \begin{cases} 0, E_{eff} \le E_c \\ \frac{\pi}{2} - 2\tan^{-1}\left[\exp\left(-\frac{E_{eff}-E_c}{30E_c}\right)\right], E_{eff} > E_c \end{cases} \tag{3}$$

Where Eeff is the effective voltage, which interacts with LC molecules and controls molecular sorting Ec is the threshold voltage, which is only related to the LC molecules itself.

*Numerical Simulation And Analysis:*

We use polyethylene as a material of PCF, which can be easily got. The refractive index of this material is 1.5. We chose the structure shown as Figure 3 and fill the marked air holes with 5CB LC. The radius of the cladding holes are 30 nm, 40 nm, 50 nm, 60 nm respectively. The air hole spacing in the cladding is 1.45mm and the input frequency is 0.7THZ.

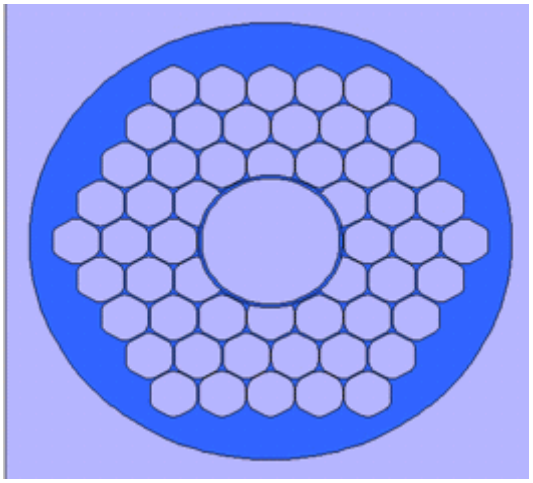

**Fig. 3:** The nematic LC schematic diagram of filling

*The Effective Refractive Index:*

The effective refractive index is an important parameter of PCF. It is closely related to other characteristics of the PCF such as chromatic dispersion. Using COMSOL Multiphysics, we can directly acquire PCF's effective refractive index in different modes. Figure 4 shows the curve of effective index varies with impressed voltage.

As what can be seen from the Figure 4, at the same applied voltage, when he hole center distance and input frequency unchanged but the pore radius increases, the fundamental mode effective index increases, and it increases more and more slowly. When the pore radius is constant, the fundamental mode effective index is proportional to the applied voltage. And the greater the voltage is, the faster the fundamental mode effective index increases. The fundamental mode effective index is proportional to the holes' radius. When pore radius is constant, the effective refractive index of the fundamental mode increases with the applied voltage increasing. The increasing trend is growing. Meanwhile, the fundamental mode effective index of four different structures does not overlap nor intersect. They almost have the same growth trend.

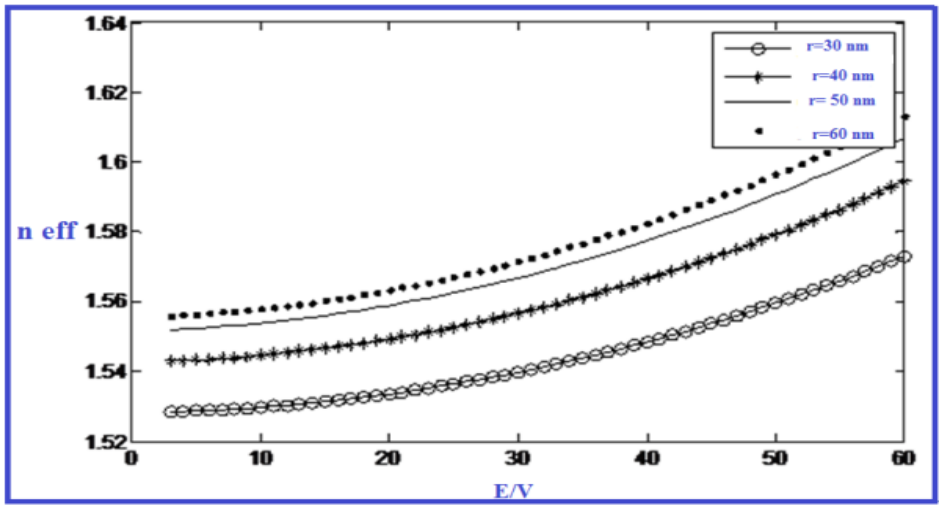


**Fig. 4:** The basic mode effective index of different aperture radius changes with the voltage

*The Normalized Frequency:*

The normalized frequency of PCF has connection with the input frequency, radius of the air holes, core effective refractive index and the cladding effective refractive index. That determined by the equation (4):

$$V_{eff} = \frac{2\pi R}{\lambda}\left(n_{core}^2 - n_{clad}^2\right)^{\frac{1}{2}} \quad (4)$$

Where define Veff <2.55 as the cut-off frequency. of second order mode. The curve of normalized frequency of PCF filled with LC versus by voltage is showed in Figure 5.

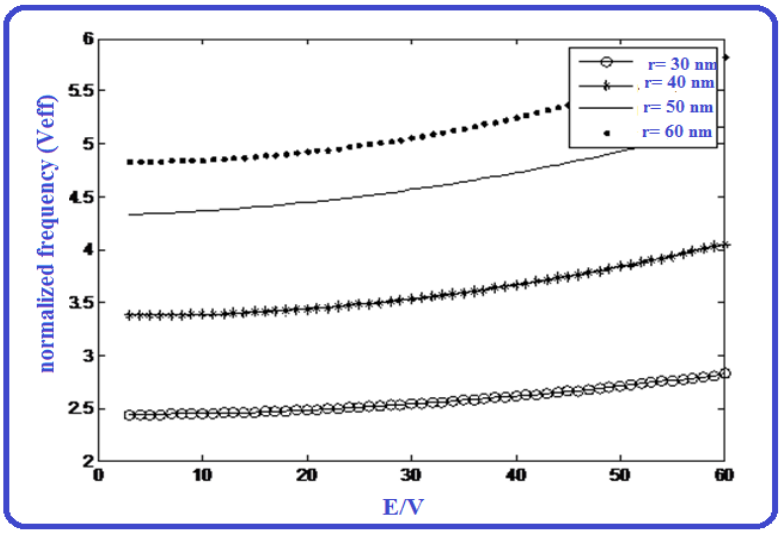


**Fig. 5:** Normalized frequency of PCF filled with LC versus voltage for different structures

Single-mode transmission can be occurring when the radius of the air holes is 30 nm and the change is gradual. The normalized frequency can be increases when the voltage is increasing. Under the same applied, Voltage the larger the radius of air holes, the larger the normalized frequency. The tendency becomes more apparent because of cladding effective refractive index changes very slowly as the voltage changing. We achieved the larger of radius of the air holes is, the less obvious change. Therefore the greater the radius of the air hole is, the effective mode has more similar curve with the effective refractive index.

*The Effective Mode Area:*

The effective mode area of PCF filled LC is measured by PCF's structure and useful voltage. We can get the large range of variation of effective mode area by choosing pertinent structure of PCF. We should project PCF with the various effective mode areas according to the required nonlinear effect. The effective mode area is demonstrated as:

$$A_{eff} = \frac{[\iint |E(x,y)|^2 dxdy]^2}{\iint |E(x,y)|^4 \, dxdy} \quad (5)$$

Here, E(x,y) represents electric mode field distribution, we select all areas of PCF materials as domain of integration.

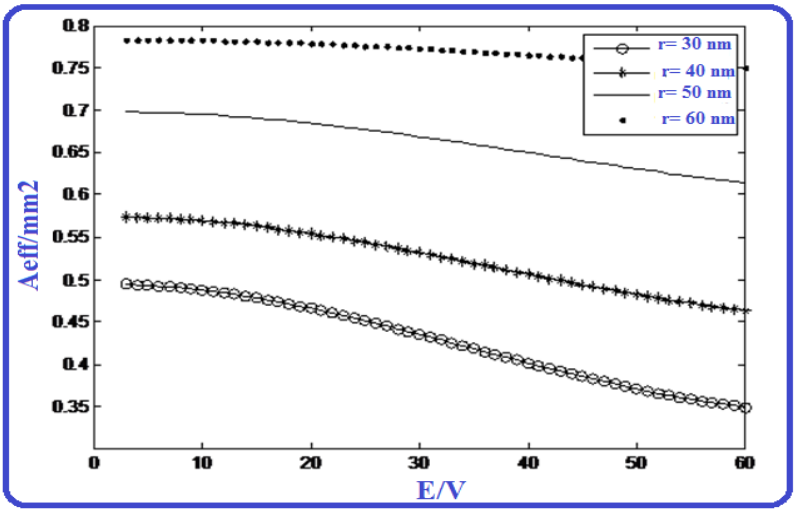


**Fig. 6:** Effective mode area of PCF filled with LC versus voltage for different structures

As shown in Figure 6, when the voltage is fixed, the mode field area increases with increase of air hole radius; when air hole radius is constant, the effective mode area increases with the applied voltage reducing. Meanwhile, the larger the radius of the air holes is effective mode area of PCF is more stable and the value of nonlinear effects is more stable. We can choose appropriate size of the structure parameters and applied voltage to control the size of the required effective mode area. And thus we can improve the nonlinear or single-mode transmission characteristics of PCF.

*Numerical Aperture:*

NA is the important parameter which react the light collecting capability of PCF, which is defined as:

$$NA = \sin\theta_a = \sin\left(\tan^{-1}\left(\frac{\lambda}{\pi\omega}\right)\right) \approx \left(1+\frac{\pi A_{eff}}{\lambda^2}\right)^{-\frac{1}{2}} \quad (6)$$

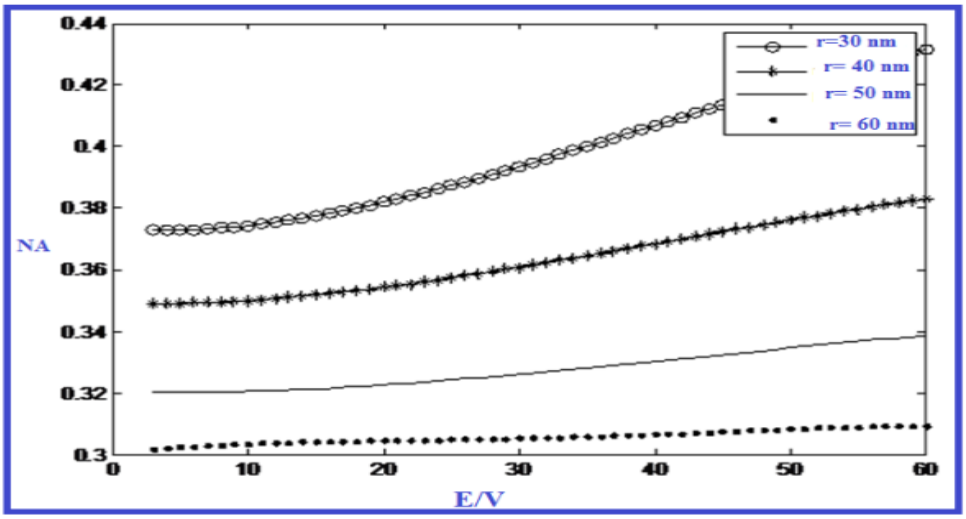


**Fig. 7:** The numerical aperture of the different aperture radius along with the change of voltage

Figure 7 shows the numerical aperture increases as the voltage amplifying when the input frequency is constant and the radius of the air hole is fixed. The numerical aperture changes gradually as the applied voltage changing and the radius of air holes increasing. The numerical aperture reduces with the radius increasing when the voltage is fixed. We can achieve the desired numerical aperture through designing different fiber structures and the adjusting applied voltage on PCF.

*Conclusion:*

In this paper, we used COMSOL and MATLAB received the performance parameters of the PCF infiltrated by LC 5CB under various voltage. These properties include effective refractive index, the normalized frequency, the effective mode area, numerical aperture, waveguide dispersion. Results indicated that both single-mode transmission and ultra-flat dispersion can be achieved under the appropriate voltage and suitable structure. Moreover, stable nonlinear effect is appeared at the large radius of air holes. It provides references to design voltage sensing terahertz waveguide device for corresponding demand.

## REFERENCES

[1] Russell, P., 2003. *Photonic crystal fibers.* science, 299(5605): 358-362.
[2] Villatoro, J., V.P. Minkovich and J. Zubia, 2014. *Locally pressed photonic crystal fiberinterferometer for multiparameter sensing.* Optics letters, 39(9): 2580-2583.
[3] Wang, W.-L., et al., 2014. *Silica cladded Nd< sup> 3+</sup>: YAG single crystal core optical fiber and its submicron residual stress detection.* Optical Materials Express, 4(4): 656-661.
[4] Mehra, R., H. Shahani and G. Kumar, 2014. *Comparison of two in-line MZI concentration sensors using FDTD method*. in *Signal Propagation and Computer Technology (ICSPCT), 2014 International Conference on*. 2014. IEEE.
[5] Bahrampour, A., et al. 2014. *Analysis of an endlessly single-mode penrose-tiling photonic quasicrystal fiber*. in *Photonics Conference, 2014 Third Mediterranean*. IEEE.

[6] Zhao, Y., Z.-q. Deng, and J. Li, 2014. *Photonic Crystal Fiber Based Surface Plasmon Resonance Chemical Sensors.* Sensors and Actuators B: Chemical.
[7] Liu, W.-J., et al., 2014. *Breathers in a hollow-core photonic crystal fiber.* Laser Physics Letters, 11(4): 045402.
[8] Prajapati, D.K. and R. Bharti, *Dispersion analysis of a Hybrid Photonic Crystal Fiber.*
[9] Saldanha, P.L., 2014. *Quantum analysis of the direct measurement of light waves.* New Journal of Physics, 16(1): 013021.
[10] Valentini, E., et al., 2014. *An effective procedure for EUNIS and Natura 2000 habitat type mapping in estuarine ecosystems integrating ecological knowledge and remote sensing analysis.* Ocean & Coastal Management.
[11] Hisatake, S., H.H.N. Pham and T. Nagatsuma, 2014. *Electric field visualization system for antenna characterization at terahertz frequency based on a nonpolarimetric self-heterodyne EO technique*. in *General Assembly and Scientific Symposium (URSI GASS), 2014 XXXIth URSI*. 2014. IEEE.
[12] Vicario, C., et al., 2014. *Intense multi-octave supercontinuum pulses from an organic emitter covering the entire THz frequency gap.* arXiv preprint arXiv: 1407.7100.
[13] Ahmad, H., et al., 2014. *Photonic crystal fiber based dual-wavelength Q-switched fiber laser using graphene oxide as a saturable absorber.* Applied Optics, 53(16): 3581-3586.
[14] Afroozeh, A., et al. 2012. *THz frequency generation using MRRs for THz imaging*. in *Enabling Science and Nanotechnology (ESciNano), 2012 International Conference on*. IEEE.
[15] Jalil, M., et al., 2012. *Generation of THz frequency using PANDA ring resonator for THz imaging.* International journal of nanomedicine, 7: 773.
[16] Afroozeh, A., et al., 2013. *THz frequency generation using Gaussian pulse for medical applications.* Optik-International Journal for Light and Electron Optics, 124(5): 416-419.
[17] Afroozeh, A., et al., 2011. *High-terahertz-frequency carrier generation by optical pulse for radio-over-fiber applications.* Optical Engineering, 50(12): 125005-125005-11.
[18] Malacarne, L.C., et al., 2014. *Role of Photophysics Processes in Thermal Lens Spectroscopy of Fluids: A Theoretical Study.* The Journal of Physical Chemistry A, 118(31): 5983-5988.
[19] Maji, P.S. and P.R. Chaudhuri, 2014. *Supercontinuum generation in ultra-flat near zero dispersion PCF with selective liquid infiltration.* Optik-International Journal for Light and Electron Optics, 125(20): 986-5992.
[20] Willman, E., et al., 2014. *Liquid crystal alignment induced by micron-scale patterned surfaces.* Physical Review E, 89(5): 052501.
[21] Wen, X., et al., 2014. *A Monte Carlo based lookup table for spectrum analysis of turbid media in the reflectance probe regime.* Quantum Electronics, 44(7): 641.
[22] Rong, Q., et al., 2014. *Polarimetric transverse strain sensor using a polarization-maintaining fiber Bragg grating mirror.*
[23] Matsui, T. and A. Okajima, 2014. *Finite-difference time-domain analysis of photonic nanojets from liquid-crystal-containing microcylinder.* Japanese Journal of Applied Physics, 53(1S): 01AE04.
[24] Ko, M.O., et al., 2014. *Dynamic measurement for electric field sensor based on wavelength-swept laser.* Optics express, 22(13): 16139-16147.
[25] Kobashi, J., et al., 2014. *Optical tuning of extraordinary optical transmission through a metallic hole array using azobenzene dye-doped nematic liquid crystal.* Japanese Journal of Applied Physics, 53(1S): 01AE02.
[26] Abass, A., et al., 2014. *Active Liquid Crystal Tuning of Metallic Nanoantenna Enhanced Light Emission from Colloidal Quantum Dots.* Nano letters.